ELSEVIER

Chemical Engineering Journal 115 (2006) 157–171

Chemical Engineering Journal

www.elsevier.com/locate/cej

Novel correlations for gas holdup in large-scale slurry bubble column reactors operating under elevated pressures and temperatures

Arsam Behkish [a], Romain Lemoine [a], Rachid Oukaci [b], Badie I. Morsi [a,*]

[a] *Chemical and Petroleum Engineering Department, University of Pittsburgh, Pittsburgh, PA 15261, USA*
[b] *Energy Technology Partners, 135 William Pitt Way, Pittsburgh, PA 15238, USA*

Received 22 October 2004; received in revised form 7 July 2005; accepted 6 October 2005

Abstract

A comprehensive literature search was conducted to obtain the holdup data for different gases in various liquids and slurries using bubble and slurry bubble column reactors operating under wide ranges of conditions in different size reactors provided with a variety of gas spargers. The data were used to develop two novel correlations, one for the total gas holdup and the other for the holdup of large gas bubbles. The total gas holdup correlation is capable of predicting the experimental data within an absolute average relative error (AARE) and standard deviation (σ) of 20%, whereas the correlation of the holdup of large bubbles is capable of predicting the experimental values within AARE and σ of about 25 and 27%, respectively. The novel correlations were used to predict the effects of pressure, temperature, gas velocity, solid concentration, rector size, and distributor type on the holdup of syngas ($H_2/CO = 2$) in various slurry bubble column reactors (SBCRs) operating under typical Fischer–Tropsch conditions.

Keywords: Bubble column reactor; Slurry bubble column reactor; Gas holdup; Holdup of large gas bubbles; Holdup of small gas bubbles; Empirical correlation; Gas distributor; Fischer–Tropsch; Modeling

1. Introduction

The gas holdup and bubbles size/distribution, among others, are strongly affected by the operating conditions in bubble column reactors (BCRs) and SBCRs and therefore their knowledge is indispensable for modeling, design and scaleup of these reactors. There are several empirical correlations available in the literature as listed in Table 1, which can be used to predict the holdup for gases in bubble columns and SBCRs, but unfortunately these correlations have several limitations and accordingly they cannot be employed to simulate the behavior of industrial-size reactors. This is because most of these correlations were developed for aqueous, highly ionic systems in small-diameter reactors operating under atmospheric pressure and/or ambient temperature; the data were obtained with different gas spargers; and the majority of the solids were non-catalytic particles. Statistical correlations have also been proposed for predicting the hydrodynamic and mass transfer parameters in two-phase and three-phase reactors and although they have been shown to enjoy high confidence levels [1], they are system-dependent and accordingly their application to predict and/or extrapolate the behavior of other gas–liquid–solid systems could be misleading [1]. Thus, adequate correlations which can be used to predict the gas holdup in multiphase reactors operating under wide ranges of industrial conditions are needed.

The objective of this study is to develop novel correlations to predict the total holdup and the holdup of large bubbles for gases in bubble columns and SBCRs operating with organic liquids, under elevated pressures and temperatures in the presence and absence of typical catalytic particles as those used in industrial applications. The effects of gas sparger design and reactor size on the gas holdup are also incorporated in these correlations.

Abbreviations: atm, atmospheric pressure; AARE, absolute average relative error $= \frac{1}{n}\sum_{1}^{n}\left|\frac{\varepsilon_{G\,Pred.}-\varepsilon_{G\,Exp.}}{\varepsilon_{G\,Exp.}}\right| \times 100$ (%); AF, acceleration factor; BC, bubble cap; BCR, bubble column reactor; DF, density factor; M-ON, multiple orifice nozzle; PfP, perforated plate; PoP, porous plate; R, ring; S, spider-type; SBCR, slurry bubble column reactor; S-ON, single orifice nozzle; SF, scale factor; SP, sintered plate

* Corresponding author.
E-mail address: Morsi@engr.pitt.edu (B.I. Morsi).

1385-8947/$ – see front matter © 2005 Elsevier B.V. All rights reserved.
doi:10.1016/j.cej.2005.10.006

Nomenclature

Bo	Bond number = $g\rho_L d^2/\sigma$
C_S	solid concentration by weight in the slurry (w/w)
C_V	volumetric solid concentration in the slurry (v/v)
d	diameter (m)
d_O	orifice diameter (m)
d_P	particle Sauter-mean diameter (m)
D_C	diameter of the column (m)
Fr	Froude number = $U_G/(gd)^{1/2}$
g	gravitational acceleration = 9.81 ($m^2\,s^{-1}$)
Ga	Galileo number = $g\rho_L^2 d^3/\mu_L^2$
H_C	height of the column (m)
K_d	gas sparger coefficient defined in Eq. (2)
M_A	molecular weight of the gas ($kg\,kmol^{-1}$)
M_B	molecular weight of the liquid ($kg\,kmol^{-1}$)
Mo	Morton number = $g\mu_L^4/(\rho_L\sigma_L)$
N_O	number of orifices in the gas sparger
P_S	vapor pressure of the liquid (MPa)
P_T	total pressure (MPa)
T	temperature (K)
U_G	superficial gas velocity ($m\,s^{-1}$)
$U_{G,O}$	superficial gas velocity at the sparger orifice ($m\,s^{-1}$)
U_L	superficial liquid velocity ($m\,s^{-1}$)
We	Weber number = $\rho_G U_{G,O}^2 d_O/\sigma_L$
X_W	weight fraction of the primary liquid in the mixture ($1 \geq X_W \geq 0.5$) (w/w)

Greek symbols

Γ	gas distributor parameter used in Eq. (1)
α	exponent defined in Eq. (2)
ε_G	gas holdup
μ	viscosity (Pa s)
ν	kinematic viscosity ($m^2\,s^{-1}$)
ρ	density ($kg\,m^{-3}$)
σ	standard deviation = $\sqrt{\frac{1}{n-1}\sum_1^n\left(\left\|\frac{\varepsilon_{G,Pred.}-\varepsilon_{G,Exp.}}{\varepsilon_{G,Exp.}}\right| - AARE\right)^2} \times 100$ (%)
σ_L	surface tension ($N\,m^{-1}$)
ζ	sparger to column cross sectional area ratio in Eq. (3) (%)

Subscripts

b	bubble
df	dense phase (small gas bubble phase)
G	gas phase
L	liquid phase
P	solid particle
SL	slurry
trans	transition from homogeneous to heterogeneous

2. Background

The hydrodynamic studies available in the literature have clearly demonstrated that the gas holdup in bubble columns and SBCRs is strongly affected by the following.

2.1. Physical properties

Gas/liquid/solid physicochemical properties include gas nature (molecular weight), liquid nature (aqueous, organic, and mixture), liquid physical properties (density, viscosity, surface tension, vapor pressure, and foaming characteristics), and solid particle nature (density and size). Ozturk et al. [18] and Inga and Morsi [19] studied the effect of gas nature on the total gas holdup and reported that under similar pressure and superficial gas velocity, the gas holdups of CO_2, air, N_2, He and H_2 in xylene and those of H_2, CO, N_2 and CH_4 in hexanes mixture, respectively appeared to follow the behavior of the molecular weight of the gas phase. Ozturk et al. [18] investigated the effect of liquid nature on the gas holdup and showed that the gas holdups of various gases (CO_2, air, N_2, He and H_2) in several organic liquids were higher than those in water. Ozturk et al. [18] and Bhaga et al. [20] studied the effect of the foaming characteristics of the liquid phase using several mixture of liquids, such as toluene and ethanol, on the gas holdup and observed a maximum in the gas holdup values at a given composition due to the formation of small gas bubbles. The effect of solid particles, including magnesium hydroxide [21], calcium hydroxide [21], iron oxide [22], calcium carbonate [23], and carbon particles [24] at various concentrations in slurry reactors was reported to increase the gas holdup and gas–liquid interfacial area at low concentrations (<5 vol.%). The increase of solid particle size, on the other hand, was found to decrease the gas holdup [25,26]. Furthermore, the effect of solid particles on the gas holdup should account not only for the solid concentration, but also for particle nature, size and density, which might significantly affect the gas holdup and subsequently the gas–liquid interfacial area [17,27].

2.2. Operating variables

These include pressure (gas density), temperature, superficial gas velocity, liquid superficial velocity, and solid concentration. Behkish et al. [28] reported that the gas holdup increases with increasing pressure, superficial gas velocity and temperature and decreases with increasing solid concentration for N_2 and He in Isopar-M using a large-scale bubble and slurry bubble column (0.29 m i.d.). The gas holdup for air in Paratherm NF using a 0.102 m i.d. column was found to insignificantly decrease with increasing the superficial liquid velocity [29]. Furthermore, Zou et al. [13] showed that at high temperatures the effect of the vapor pressure becomes significant and consequently the actual gas density should be corrected for. Nonetheless, the dependency of the total gas holdup on the superficial gas velocity was mainly a strong function of the prevailing hydrodynamic flow regime [30].

Table 1
Gas holdup correlations available in the literature

Authors	Gas/liquid/solid system	Experimental conditions	Correlation
Bach and Pilhofer [2]	Air/alcohol, hydrocarbons	P atm., T: ambient, U_G: 0–0.2 m/s	$\frac{\varepsilon_G}{1-\varepsilon_G} = 0.115\left(\frac{U_G^3}{\nu_L g(\rho_L-\rho_G)/\rho_L}\right)^{0.23}$
Hikita et al. [3]	Air, H_2, CO_2, CH_4, C_3H_8/H_2O, 30, 50 wt.% sucrose, methanol, n-butanol, aniline	P: atm., T: ambient, U_G: 0.042–0.38 m/s, D_C: 0.1 m, H_C: 1.5 m	$\varepsilon_G = 0.672\left(\frac{U_G\mu_L}{\sigma_L}\right)^{0.578}\left(\frac{\mu_L^4 g}{\rho_L\sigma_L^3}\right)^{-0.131}\left(\frac{\rho_G}{\rho_L}\right)^{0.062}\left(\frac{\mu_G}{\mu_L}\right)^{0.107}$
Hughmark [4]	Air/H_2O, kerosene, oil, Na_2CO_3 and $ZnCl_2$ aqueous sol, Glycerol, light oil	P: atm., T: ambient, U_G: 0.004–0.45 m/s, D_C: 0.0254 m	$\varepsilon_G = \frac{1}{2+\left(\frac{0.35}{U_G}\right)\left(\frac{\rho_L\sigma_L}{72}\right)^{1/3}}$
Idogawa et al. [5]	H_2, He, air/H_2O, CH_3OH, C_2H_5OH, acetone, aqueous alcohol solutions	P: 0.1–5 MPa, T: ambient, U_G: 0.005–0.05 m/s	$\frac{\varepsilon_G}{1-\varepsilon_G} = 0.059U_G^{0.8}\rho_G^{0.17}\left(\frac{\sigma_L}{72}\right)^{-0.22\exp(-P)}$, σ_L (mN/m), U_G (cm/s)
Jordan and Schumpe [6]	N_2, He/ethanol, 1-butanol, toluene, decalin	P: 0.1–4 MPa, T: 293–343 K, U_G: 0.01–0.21 m/s, D_C: 0.1 m, H_C: 2.4 m	$\frac{\varepsilon_G}{1-\varepsilon_G} = bBo^{0.16}Ga^{0.04}Fr^{0.70}\left(1+27.0\,Fr^{0.52}\left(\frac{\rho_G}{\rho_L}\right)^{0.58}\right)$, Dimensionless numbers based on the bubble diameter, b depends on the sparger: 19 × 1 mm PfP = 0.112, 1 × 1 mm PfP = 0.122, 1 × 4.3 mm PfP = 0.109, 3 mm S-ON = 0.135, 7 × 1 mm PfP = 0.153
Krishna and Ellenberger [7]	Air/H_2O, H_2O + Separan, paraffin oil, tetradecane	P: atm., T: ambient, U_G: 0.001–0.866 m/s, D_C: 0.1, 0.174, 0.19, 0.38, 0.63 m	$\varepsilon_G = \varepsilon_{G\text{-Large}} + \varepsilon_{df}(1-\varepsilon_{G\text{-large}})$, $\varepsilon_{df} = 0.59\times(3.85)^{1.5}\sqrt{\frac{\rho_G^{0.96}\sigma_L^{0.12}}{\rho_L}}$, $\varepsilon_{G\text{-Large}} = 0.268\times D_C^{-0.18}\frac{(U_G-U_{G-df})^{4/5}}{(U_G-U_{G-df})^{0.22}}$, $U_{G\text{-df}} = U_{b\text{-Small}}\varepsilon_{df}(1-\varepsilon_{df})$, $U_{b\text{-Small}} = \frac{\sigma_L^{0.12}}{2.84\rho_G^{0.04}}$
Kumar et al. [8]	Air/H_2O, glycerol, kerosene	P: atm., T: ambient, U_G: 0.0014–0.14 m/s	$\varepsilon_G = 0.728U - 0.485U^2 + 0.0975U^3$, $U = U_G[\rho_L^2/\sigma_L(\rho_L-\rho_G)g]^{1/4}$
Reilly et al. [9]	Air/H_2O, solvent, TCE/glass	P: atm., T: ambient, U_G: 0.02–0.2 m/s, C_V: up to 10 vol.%, D_C: 0.3 m, H_C: 5 m	$\varepsilon_G = 296U_G^{0.44}\rho_L^{-0.98}\sigma_L^{-0.16}\rho_G^{0.19} + 0.009$
Reilly et al. [10]	Air, N_2, He, Ar, CO_2/Isopar-G, Isopar-M, TCE, Varsol, H_2O	P: up to 1.1 MPa, T: ambient, U_G: 0.006–0.23 m/s, D_C: 0.15 m, H_C: 2.7 m	$\varepsilon_G = A\frac{\rho_G U_G}{\rho_L(1-\varepsilon_G)}$ (homogeneous flow regime), $\varepsilon_G = B\left(\frac{\rho_G U_G}{\rho_L(1-\varepsilon_G)}\right)^{1/3}$ (heterogeneous flow regime), A and B depend on the liquid nature, $A = 2.84\rho_L\rho_G^{-0.96}\sigma_L^{-0.12}$, B = 3.8 (Isopar-G: ρ_L = 740, μ_L = 0.000861, σ_L = 0.0235), 3.7 (Isopar-M: ρ_L = 779, μ_L = 0.002433, σ_L = 0.0266), 3.6 (TCE: ρ_L = 1462, μ_L = 0.000572, σ_L = 0.03), 4.6 (Varsol: ρ_L = 773, μ_L = 0.001012, σ_L = 0.0283), 4 (H_2O: ρ_L = 1000, μ_L = 0.001, σ_L = 0.0728)
Urseanu et al. [11]	N_2/Tellus oil, glucose solutions	P: 0.1–1 MPa, T: ambient, U_G: up to 0.3 m/s, D_C: 0.15, 0.23 m, H_C: 1.22 m	$\varepsilon_G = 0.21U_G^{0.58}\mu_L^{-0.12}\rho_G^{[0.3\exp(-9\mu_L)]}$
Wilkinson et al. [12]	N_2/n-heptane, mono-ethylene glycol, H_2O	P: up to 1.5 MPa, T: ambient, U_G: up to 0.3 m/s, D_C: 0.158 m, H_L: 1.5 m	$\varepsilon_G = \frac{U_{trans}}{U_{b\text{-Small}}} + \frac{U_G-U_{trans}}{U_{b\text{-Large}}}$, $U_{b\text{-Small}} = 2.25\frac{\sigma_L}{\mu_L}\left(\frac{\sigma_L^3\rho_L}{\mu_L^4 g}\right)^{-0.273}\left(\frac{\rho_L}{\rho_G}\right)^{0.03}$, $U_{trans} = 0.5\times U_{b\text{-small}}\exp(-193\rho_G^{-0.61}\mu_L^{0.5}\sigma_L^{0.11})$, $U_{b\text{-Large}} = U_{b\text{-Small}} + 2.4\frac{\sigma_L}{\mu_L}\left(\frac{\mu_L(U_G-U_{trans})}{\sigma_L}\right)^{0.757}\left(\frac{\sigma_L^3\rho_L}{g\mu_L^4}\right)^{-0.077}\left(\frac{\rho_L}{\rho_G}\right)^{0.077}$
Zou et al. [13]	Air/H_2O, alcohol, 5% NaCl	P: atm., T: 298–370 K, U_G: 0.01–0.16 m/s, U_L: 0.007 m/s, D_C: 0.1 m, H_C: 1.05 m	$\varepsilon_G = 0.17283\left(\frac{\mu_L^4 g}{\rho_L\sigma_L^3}\right)^{-0.1544}\left(\frac{P_T+P_S}{P_T}\right)^{1.6105}\left(\frac{U_G\mu_L}{\sigma_L}\right)^{0.5897}$

Table 1 (*Continued*)

Authors	Gas/liquid/solid system	Experimental conditions	Correlation
Fan et al. [14]	N_2/paratherm NF/alumina	P: 0.1–5.62 MPa, T: 301 and 351 K, U_G up to 0.45 m/s, C_V: 8.1, 19.1 vol.%, D_C: 0.102 m, H_C: 1.37 m	$\frac{\varepsilon_G}{1-\varepsilon_G} = \frac{2.9(U_G^4\rho_G/\sigma_L g)^{\alpha}(\rho_G/\rho_{SL})^{\beta}}{[\cosh(Mo_{Sl}^{0.054})]^{4.1}}$, $Mo_{SL} = g(\rho_{SL}-\rho_G)(\xi\mu_L)^4/\rho_{SL}^2\sigma_L^3$, $\alpha = 0.21Mo_{Sl}^{0.0079}$ and $\beta = 0.096\,Mo_{Sl}^{-0.011}$, $\mathrm{Ln}\,\xi = 4.6C_V\{5.7C_V^{0.58}\sinh[-0.71\exp(-5.8C_V)\ln Mo^{0.22}] + 1\}$
Krishna and Sie [15]	Air/paraffin oil, Tellus oil/silica	P: atm., T: ambient, U_G: up to 0.5 m/s, C_V: 0–36 vol.%, D_C: 0.1, 0.19, 0.38, 0.63 m	$\varepsilon_G = \varepsilon_{G\text{-Large}} + \varepsilon_{df}(1-\varepsilon_{G\text{-Large}})$, $\varepsilon_{G\text{-Large}} = \frac{U_G - U_{G-df}}{U_{b\text{-Large}}}$, $U_{b\text{-Large}} = 0.71\sqrt{gd_b}(SF)(AF)(DF)$, $SF = 1$ for $d_b/D_C < 0.125$, $SF = 1.13\exp\left(-\frac{d_b}{D_C}\right)$, for $0.125 < d_b/D_C < 0.6$ $SF = 0.496\sqrt{\frac{D_C}{d_b}}$ for $d_b/D_C > 0.6$, $AF = \alpha + \beta(U_G - U_{G\text{-df}})$, $DF = \sqrt{1.29/\rho_G}$, $d_b = \gamma(U_G - U_{G\text{-df}})^{\delta}$, for Tellus oil ($\rho_L = 862$, $\mu_L = 0.075$, $\sigma_L = 0.028$), $\alpha = 2.25$, $\beta = 4.09$, $\gamma = 0.069$, $\delta = 0.376$, $U_{G-df} = U_{b-small}\varepsilon_{df}$, $\varepsilon_{df} = \varepsilon_{df,0}\left(\frac{\rho_G}{\rho_{G,ref}}\right)^{0.48}\left(1 - \frac{0.7}{\varepsilon_{df,0}}C_V\right)$, $\varepsilon_{df,0} = 0.27$ for paraffin oil ($\rho_L = 790$, $\mu_L = 0.029$, $\sigma = 0.028$), $U_{b-small} = U_{b-small,0}\left(1 + \frac{0.8}{U_{b-small,0}}C_V\right)$, $U_{b\text{-Small},0} = 0.095$ m/s for paraffin oil
Sauer and Hempel [16]	Air/H_2O/10 diff. solids ($1020 < \rho_P < 2780$ kg/m^3)	P: atm., T: ambient, U_G: 0.01–0.08 m/s, C_V: 0–20 vol.%	$\frac{\varepsilon_G}{1-\varepsilon_G} = 0.0277\left(\frac{U_G}{(U_G g\nu_{sl})^{0.25}}\right)^{0.844}\left(\frac{\nu_{sl}}{\nu_{eff,rad}}\right)^{-0.136}\left(\frac{C_s}{C_{S0}}\right)^{0.0392}$ where C_{S0} is solid concentration at bottom of column (kg/m^3), $\nu_{Sl} = \mu_L[1 + 2.5C_V + 10.05C_V^2 + 0.00273\exp(16.6C_V)]/\rho_{SL}$, $\nu_{eff,rad} = 0.011D_C\sqrt{gD_C}\left(\frac{U_G^3}{g\nu_L}\right)^{1/8}$
Schumpe et al. [17]	N_2, O_2/H_2O, 0.8 M Na_2SO_4/carbon, Kieselguhr, aluminum oxide	P: atm., T: ambient, U_G: up to 0.07 m/s, C_S: up to 300 kg/m^3, D_C: 0.095 m, H_C: 0.85 m	$\varepsilon_G = BU_G^{0.87}\mu_{eff}^{-0.18}$, $\mu_{eff} = k(2800U_G)^{n-1}$ k and n are F (C_V, solid nature), $B = 0.81$ or 0.43, $0.89 \le 10^3\,k$ (Pa s^n) ≤ 1730, $0.163 \le n \le 1$

2.3. Reactor size

It has been reported that the hydrodynamics of SBCRs are strongly dependent on the column geometry as well as the gas distribution technique [30]. In fact, based on the column geometry, the following three different regions with their respective gas holdup were identified [12,31]: (1) sparger region (ε_G depends on the gas distributor design); (2) bulk region (ε_G is controlled by the liquid/slurry circulation); (3) top region (ε_G is large due to the formation of a layer of froth above the liquid/slurry bed). In general, the gas holdup will then be the sum of the holdups in the three regions, however, if the column is long enough, the influence of the first and third regions on the gas holdup will be insignificant and thus the gas holdup will be close to the values measured in the bulk region [12]. The ratio of height of the reactor to its diameter (H_C/D_C) would therefore affect the gas holdup. A number of investigators reported that typically no obvious change in the gas holdup was observed when H_C/D_C ratios were >5–6 [12,35,32], as the effect of sparger on the total gas holdup within the top region of the reactor was insignificant. Furthermore, the gas holdup was found to decrease with column diameter [33] due to a reduction in the holdup of large gas bubbles [15,34], a change in the liquid backmixing [30], and a reduction of the foaming ability of the liquid/slurry [35]. A few investigators have also observed that with highly viscous liquid (i.e. $\geq$0.55 Pa s), the effect of column diameter on ε_G was more pronounced due to a weak wall effect on the rise velocity of the gas bubbles [11,36]. Koide et al. [37] measured the gas holdup of air/water system in the churn-turbulent flow regime and reported that ε_G values obtained in a 0.218 and 0.3 m i.d. columns were identical but systematically lower that those obtained in a 0.1 and 0.14 m i.d. column. Similarly, many investigators have reported that the ε_G would level off when column diameters are $\geq$0.15 m [12,32,38,39]. Koide et al. [40] measured the gas holdup and bubble sizes of air in water in a 5.5 m i.d. column and compared their data with those obtained in smaller columns (0.1–0.6 m i.d.) and although they observed a small influence of the column diameters on the ε_G, they suggested that the difference was negligible [40]. They further reported, however, that the arithmetic mean bubble diameter measured in their column was higher than those calculated with correlations developed for smaller diameter columns, and attributed this behavior to the breakup and coalescence of gas bubbles along with gas dispersion which were affected by the design and geometry of their column [40]. In addition, they hinted that if larger gas bubbles were formed in larger columns, a relatively smaller total

gas holdup would be expected. Thus, since most commercial SBCRs have inside diameters greater than 5 m [15], to conclude that the gas holdup will remain constant from a diameter of $0.15 - \geq 5$ m could be inaccurate. The careful approach would be to consider that the gas holdup continues to slightly decrease at column diameters >0.15 m and slowly reaches an asymptote depending on the operating variables, physicochemical properties of the gas–liquid system and the geometries of the column and gas sparger.

2.4. Gas distributor

Gas distributors are integral part of the design and scale-up of bubble columns and SBCRs. There are numerous types of gas distributor (i.e. spider, perforated plate, sintered plate, nozzles, etc.), which significantly differ in their size and number of orifices. Among the most commonly used gas distributors are perforated plates, porous plates, sintered plates, single-orifice nozzles, multiple-orifice nozzles, rings, spider types, bubble caps, injector and ejector types. The characteristics of a gas distributor include, among others, opening size, number of openings, sparger positioning, and nozzles position/orientation. The initial bubble size and distribution at the orifice could be controlled by the sparger characteristics, nevertheless, Akita and Yoshida [41] reported that due to the balance between coalescence and breakup of gas bubbles, the initial bubble size created at the gas sparger would not describe the behavior of gas bubble size distribution in the entire bubble column. The effect of gas sparger on the gas holdup is considered complex [30,42], since its influence beyond the sparger zone is yet to be understood. Several investigators have reported that gas sparger had a minimal effect on the bubble sizes and gas holdup if the orifice diameters were >1–2 mm [12,32,41]. Jordan and Schumpe [6], however, took into account the effect of gas sparger on the gas holdup even though the orifice diameters of each of their three perforated plates were either equal or greater than 1 mm, and despite the fact that no considerable effect of the gas spargers on ε_G was observed [6]. It should be mentioned that the quality of the gas holdup (small versus large) depends on the breakup and coalescence of the gas bubbles in the column. Porous plates, with relatively smaller pore diameters, have been found to generate smaller gas bubbles when compared to those by perforated plates [12]. Also, single orifice nozzles, with diameters usually greater than 0.001–0.002 m, generated large gas bubbles, even at very low superficial gas velocity [41] indicating a heterogeneous bubble size distribution [43]. From these observations, one can conclude the ε_G is inversely proportional to the orifice diameter, and when small gas bubbles are formed, the transition from homogeneous to heterogeneous flow regime is delayed, since the rate of bubble coalescence becomes smaller [43]. An important effect of the gas distributors on ε_G was observed by Schügerl et al. [44] when they separately added 10 wt.% sodium sulfate (Na_2SO_4) and 1% ethanol to water to obtain a non-coalescing system. The authors reported that under these conditions, the smallest gas holdup was measured with the perforated plate ($d_O = 5 \times 10^{-4}$ m), followed by the sintered plate ($d_O = 17.5 \times 10^{-6}$ m), the injector type ($d_O = 4 \times 10^{-3}$ m), and the ejector type ($d_O = 3 \times 10^{-3}$ m). It seems that the two jet-model spargers have systematically provided higher gas holdup values than those with the perforated and sintered plates, despite their larger orifice diameters. The reason for this behavior was attributed to the authors' unique mechanism of creating large gas–liquid interface by mixing the gas and the liquid prior to the injection into the column [30]. Furthermore, Schügerl et al. showed that in a coalescing system (i.e. H_2O) the effect of gas distributor on the ε_G values was not significant, confirming that in a non-coalescing system, the bubble size distribution is controlled by the gas distributor [42,44]. Thus, if the gas/liquid system in a bubble column or SBCR is non-coalescing, one can expect that the bubble size distribution and subsequently the gas holdup would be strongly dependent on the gas distributor design.

Table 2
Values of K_d used in Eq. (2)

Distributor	K_d
R, S	1.000
S-ON	1.205
PfP, M-ON	1.364
BC, PoP, SP	1.553

3. Novel correlations development

From this background, it seems that any correlation to be developed for predicting the gas holdup in bubble columns and slurry bubble column reactors has to account for the impact of the above mentioned criteria, including pressure, temperature, gas superficial velocity, solid concentration, particle density/concentration, rector size, gas sparger characteristics, etc. In this study, the total gas holdup (ε_G) data measured in our laboratories along with those obtained from the literature references listed in Table 2, totaling 3881 data points were used to develop the following correlation:

$$\varepsilon_G = 4.94 \times 10^{-3} \times \left(\frac{\rho_L^{0.415}\rho_G^{0.177}}{\mu_L^{0.174}\sigma_L^{0.27}}\right) U_G^{0.553} \left(\frac{P_T}{P_T - P_S}\right)^{0.203} \times \left(\frac{D_C}{D_C + 1}\right)^{-0.117} \Gamma^{0.053} \times \exp[-2.231 C_V - 0.157(\rho_P d_P) - 0.242 X_W] \quad (1)$$

Γ represents the effect of the gas sparger type, can be calculated from

$$\Gamma = (K_d \times N_O d_O^{\alpha}) \quad (2)$$

$$\zeta = N_O \left(\frac{d_O}{D_C}\right)^2 \times 100 \quad (3)$$

In Eq. (2), K_d is the distributor coefficient, N_O is the number of orifices in the sparger, and d_O is the diameter of the orifice. The values of K_d are given in Table 2 and the exponent α for several distributors can be found in Table 3. For perforated plates,

Table 3
Value of α used in Eq. (2)

Distributor	ζ (%)	α
PfP	<0.055	0.017
PfP	≥0.055 and ≤0.3	0.303
PfP	>0.3	0.293
M-ON		0.303
S-ON		0.134
R, S		0.015
BC		0.500
PoP, SP		0.650

however, the exponent α should be obtained from ζ, defined by Eq. (3).

X_W in Eq. (1) represents the concentration of the primary liquid in a binary mixture, and its value lies between 0.5 and 1. It should be mentioned that for a single-component or an organic liquid mixture, consisting of several hydrocarbons, such as oils and waxes, X_W equals 1. Also, in the case of bubble column reactors, C_V, ρ_P, and d_P are zeros. Thus, Eq. (1) considers the effects of gas–liquid–solid properties, liquid-phase composition, operating conditions, gas sparger type, and column diameter on the total gas holdup. Table 4 presents the ranges of the conditions of applicability of Eq. (1). It should be mentioned, however, that in an attempt to incorporate all the variables affecting the gas holdup into a nonlinear regression scheme, Eqs. (1) and (2) came to be dimensional.

Fig. 1 shows a comparison between predicted and our experimental gas holdup values along with those obtained from the literature references listed in Table 5, and as can be seen the agreement between the predicted and experimental values is within an absolute average relative error (AARE) and a standard of deviation (σ) of 20%.

The importance of Eq. (1) lies in the fact that it allows predicting the total gas holdup for a single-component as well as a multi-component gaseous system in liquids and/or slurries provided that the gas density under given operating conditions is known. For this purpose an equation-of-state (EOS), such as Peng–Robinson EOS can be employed to determine the gas density which then can be used along with other needed variables in Eq. (1) to predict the corresponding total gas holdup.

Table 4
Upper and lower limits of the variables involved in Eq. (1)

Variables	Minimum value	Maximum value
P_T (MPa)	0.1	15
P_S (MPa)	0	0.7
U_G (m/s)	3.5×10^{-3}	0.574
C_v (vol.%)	0	36
X_w	0.5	1.0
T (K)	275	538
M_B (kg/kmol)	18	730
M_A (kg/kmol)	2	44
dp ($\times 10^{-6}$ m)	5	300
ρ_P (kg/m^3)	700	4000
ρ_G (kg/m^3)	0.06	177.3
ρ_L (kg/m^3)	633.4	1583
μ_L ($\times 10^{-3}$ Pa s)	0.189	398.8
σ_L ($\times 10^{-3}$N/m)	8.4	75
D_C (m)	0.0382	5.5

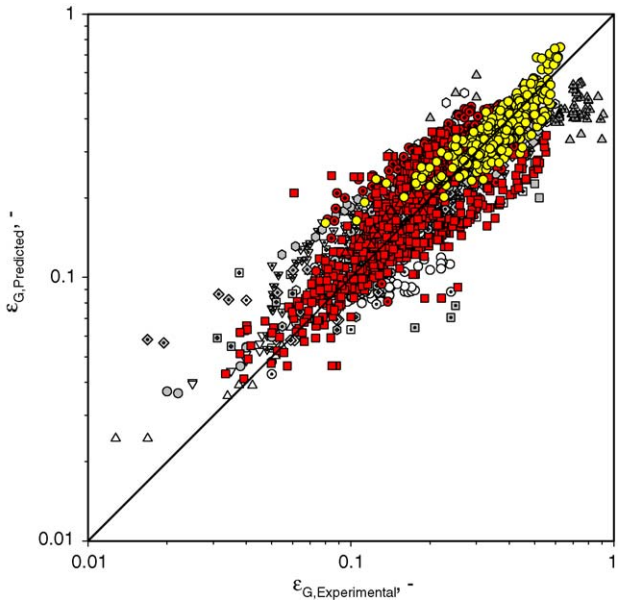

Fig. 1. Comparison between predicted and experimental total gas holdup data using Eq. (1).

It should be emphasized that BCRs and SBCRs operating in the churn-turbulent flow regime, small and large gas bubbles were reported to coexist [1,15,19,28]; Eq. (1) is valid for predicting the total holdup of all the gas bubbles present. The large gas bubbles rise in the reactor in a plug-flow whereas the small bubbles are back-mixed within the liquid or slurry. In this study, large gas bubbles were arbitrarily defined as those having a Sauter mean bubble diameters >0.0015 m, as photographically observed by Behkish et al. [28]. In order to determine the gas holdup corresponding to large bubbles ($\varepsilon_{G\text{-Large}}$), our experimental holdup data of large gas bubbles along with those obtained from the literature references given in Table 6, totaling 1426 data points were used to develop the following correlation:

$$\varepsilon_{G\text{-Large}} = \varepsilon_G^{0.84}\left(1 - 3.04 \times 10^{-6}\frac{\rho_L^{0.97}}{\mu_L^{0.16}}e^{4.50X_W - 4.59C_V}\right) = \varepsilon_G^{0.84}(F) \quad (4)$$

Fig. 2 depicts a comparison between experimental and predicted holdup data of large gas bubbles using Eq. (4); as can be observed the agreement between the values is within an absolute average relative error (AARE) and a standard of deviation (σ) of about 23 and 27%, respectively.

Thus, from the knowledge of the total gas holdup (ε_G), Eq. (1) and the holdup of large gas bubbles, Eq. (4), the holdup of small gas bubbles ($\varepsilon_{G\text{-Small}}$) can be deduced as

$$\varepsilon_{G\text{-Small}} = \varepsilon_G - \varepsilon_{G\text{-Large}} \quad (5)$$

It should be noted that coupling Eqs. (1) and (4) leads to the following situations:

Table 5
Available literature data on the total gas holdup used in the development of Eq. (1)

Author	Gas	Liquid	Solid	Operating variables	D_C (m)	Sparger	Symbols
Bhaga et al. [20]	N_2	*n*-Octane + toluene, cumene + ams, toluene + ethanol, toluene + ams, toluene + cumene, toluene + ethylbenzene, acetone + benezene	–	*P*: atm., *T*: 298, 333 K, U_G: 0.0213–0.035 m/s	0.0382	PfP	
Bukur et al. [45]	O_2	Wax	–	*P*: atm., *T*: 473, 538 K, U_G: 0.01–0.15 m/s	0.229	PfP	
Camarasa et al. [43]	Air	H_2O	–	*P*: atm., *T*: ambient, U_G: 0.013–0.15 m/s	0.1	PoP	
Chabot and Lasa [46]	N_2	Paraffin oil	–	*P*: atm., *T*: 373, 448 K, U_G: 0.022–0.146 m/s	0.2	PfP	
Daly et al. [47]	Air	Sasol wax	–	*P*: atm., *T*: 538 K, U_G: 0.02–0.12 m/s	0.05	PfP	
Dewes et al. [48]	Air	H_2O-0.8 M sodium sulfate	–	*P*: 0.1–0.8 MPa, *T*: ambient, U_G: 0.03–0.08 m/s	0.115	PfP	
Eickenbusch et al. [36]	Air	H_2O + hydroxypropyl guar	–	*P*: atm., *T*: ambient, U_G: 0.0095–0.09 m/s	0.19, 0.29, 0.6	PfP, R	
Grover et al. [49]	Air	H_2O	–	*P*: atm., *T*: 303–353 K, U_G: 0.012–0.041 m/s	0.1	SP	
Grund et al. [50]	Air	H_2O, methanol, toluene, ligroin	–	*P*: atm., *T*: 293 K, U_G: 0.1025–0.1946 m/s	0.15	PfP	
Halard [51]	Air	H_2O-CMC sol	–	*P*: atm, *T*: ambient, U_G: 0.02–0.05 m/s	0.76	R	
Jiang et al. [52]	N_2	Paratherm NF	–	*P*: 0.1–12.2 MPa, *T*: ambient U_G: 0.027–0.075 m/s	0.0508	R	
Jordan and Schumpe [6]	N_2, He	Ethanol, decalin, 1-butanol, toluene	–	*P*: 0.1–4 MPa, *T*: 293, 343 K, U_G: 0.021–0.22 m/s	0.1	PfP	
Kataoka et al. [53]	CO_2	H_2O	–	*P*: atm., *T*: ambient, U_G: 0.021–0.05 m/s	5.5	M-ON	
Laari et al. [54]	Air	H_2O	–	*P*: atm., *T*: ambient, U_G: 0.018–0.038 m/s	0.98	S-ON	
Lau et al. [29]	Air	Paratherm NF	–	*P*: 0.1–4.24 MPa, *T*: 298, 365 K, U_G: 0.019–0.039 m/s, U_L: 0.0008–0.0032 m/s	0.1016	PfP	
Lemoine et al. [1]	N_2, air	Toluene, toluene + benzoic acid + benzaldehyde	–	*P*: 0.182–0.82 MPa, *T*: ambient, U_G: 0.056–0.15 m/s	0.316	S	
Letzel et al. [55]	N_2	H_2O	–	*P*: 0.1–0.9 MPa, *T*: ambient, U_G: 0.12–0.2 m/s	0.15	PfP	
Moujaes [56]	N_2, air	Tetraline, H_2O, ethylene glycol	–	*P*: atm., *T*: 275–293 K, U_G: 0.0152–0.1173 m/s	0.127, 0.3048, 1.8288	S-ON, M-ON	
Ozturk et al. [18]	Air, CO_2, N_2, He, H_2	Xylene, *p*-xylene, toluene + ethanol, ligroin, ethylbenzene, ethylacetate, CCl_4, 1,4-dioxane, acetone, nitrobenzene, 1,2-dichloroethane, aniline	–	*P*: atm., *T*: 293 K, U_G: 0.03–0.082 m/s	0.095	S-ON	
Pino et al. [57]	Air	Kerosene	–	*P*: atm., *T*: 298 K, U_G: 0.1–0.175 m/s	0.29	PfP	
Pohorecki et al. [58]	N_2	Cyclohexane	–	*P*: 1.1 MPa, *T*: 373–433 K, U_G: 0.0035 m/s	0.304	M-ON	
Saxena et al. [25]	Air	H_2O	–	*P*: atm., *T*: 343, 353 K, U_G: 0.01–0.3 m/s	0.305	BC	

Table 5 (*Continued*)

Author	Gas	Liquid	Solid	Operating variables	D_C (m)	Sparger	Symbols
Shah et al. [59]	Air	H_2O + ethanol	–	*P*: atm., *T*: ambient, U_G: 0.1058–0.2083 m/s	0.1	SP	
Syeda et al. [60]	Air	Methanol + propanol, ethyleneglycol + H_2O, propanol + H_2O	–	*P*: atm., *T*: ambient, U_G: 0.32 m/s	0.09	PfP	
Tarmy et al. [61]	N_2	*n*-Heptane	–	*P*: 0.12–0.62 MPa, *T*: ambient, U_G: 0.12 m/s	0.61	S-ON	
Towell et al. [62]	CO_2	H_2O	–	*P*: atm., *T*: 300 K, U_G: 0.07 m/s	0.407	S-ON	
Veera et al. [63]	Air	H_2O	–	*P*: atm., *T*: ambient, U_G: 0.06–0.29 m/s	0.385	PfP, S-ON	
Wezorke [64]	Air	Mono-ethylene glycol	–	*P*: atm., *T*: ambient, U_G: 0.11–0.41 m/s	0.44	S-ON	
Wilkinson et al. [65]	N_2	0.8 M sodium sulfite + H_2O, H_2O, mono-ethylene glycol, *n*-heptane	–	*P*: 0.1–2 MPa, *T*: 293 K, U_G: 0.03–0.28 m/s	0.15, 0.158, 0.23	R	
Zou et al. [13]	Air	H_2O, ethanol	–	*P*: atm., *T*: 313–369.5 K, U_G: 0.04–0.166 m/s, U_L: 0.007 m/s	0.1	S-ON	
Deckwer et al. [66]	N_2	Wax	Al_2O_3	*P*: 0.4 MPa, *T*: 523 K, U_G: 0.0044–0.034 m/s, C_V: 0–1.21 vol.%	0.1	SP	
Luo et al. [67]	N_2	Paratherm NF	Alumina	*P*: 0.1–2.86 MPa, *T*: 301 K, U_G: 0.04–0.333 m/s, C_V: 0–19.1 vol.%	0.102	PfP	
Kluytmans et al. [24]	N_2	H_2O	Carbon	*P*: atm., *T*: ambient, U_G: 0.04–0.11 m/s, C_V: 0–1.429×10^{-3} vol.%	0.3	PfP	
Choi et al. [68]	Air	H_2O	Glass beads	*P*: atm., *T*: ambient, U_G: 0.0205–0.08 m/s, C_V: 3 vol.%	0.456×0.153	PfP	
Gandhi et al. [69]	Air	H_2O	Glass beads	*P*: atm., *T*: ambient, U_G: 0.05–0.26 m/s, C_V: 10–35 vol.%	0.15	S	
Li et al. [70]	Air	H_2O	Glass beads	*P*: atm., *T*: ambient, U_G: 0.05–0.3 m/s	0.28	S	
O'Dowd [71]	N_2	H_2O	Glass beads	*P*: atm., *T*: ambient, U_G: 0.031–0.194 m/s, C_V: 4.17–10.74 vol.%	0.108	PfP	
Inga and Morsi [19]	H_2, CO, CH_4, N_2	Hexanes	Iron oxides	*P*: 0.126–0.767 MPa, *T*: ambient, U_G: 0.06–0.35 m/s, C_V: 0–21.76 vol.%	0.316	S	
Godbole [72]	Air	H_2O, H_2O + CMC, H_2O + 0.8 M sodium sulfite, H_2O + ethanol, H_2O + propanol, H_2O + butanol, H_2O + methanol, H_2O +glycerine, Sotrol-130	Polystyrene, coal, oil shell, sand	*P*: atm., *T*: 298 K, U_G: 0.017–0.57 m/s, C_V: 0–26.3 vol.%	0.305	PfP	
Krishna et al. [34]	Air	Paraffin oil	Silica	*P*: atm., *T*: ambient, U_G: 0.085–0.2175 m/s, C_V: 0–36 vol.%	0.38	SP	
Behkish et al. [28]	N_2, He	Isopar-M	Alumina	*P*: 0.7-3.0 MPa, *T*: 300–453 K, U_G: 0.07–0.39 m/s, C_V: 0–20 vol.%	0.29	S	

Table 6
Available literature data on the holdup of large gas bubbles used in the development of Eq. (4)

Authors	Gas	Liquid	Solid	Operating variable	D_C (m)	Sparger	Symbol
Ellenberger and Krishna [73]	Air, Ar, He, SF_6	Water, tetradecane, paraffin oil	–	P: atm., T: 298 K, U_G: 0.06–0.7 m/s	0.10, 0.19, 0.38	SP	
Grund et al. [50]	Air	Water, methanol, toluene, ligroin	–	P: atm., T: 293 K, U_G: 0.103–0.195 m/s	0.15	PfP	
Hyndman et al. [74]	Air, Ar	Water	–	P: atm., T: ambient, U_G: 0.04–0.15 m/s	0.20	PfP	
Jordan et al. [75]	N_2, He	Ethanol, decalin, 1-butanol, toluene	–	P: 0.1–4.0 MPa, T: 293 K, U_G: 0.01–0.22 m/s	0.1	PfP, PoP	
Lemoine et al. [1]	N_2, air	Toluene, toluene + benzoic acid + benzaldehyde	–	P: 0.18–0.82 MPa, T: ambient, U_G: 0.056–0.15 m/s	0.316	S	
Vermeer and Krishna [76]	Air	Turpentine 5	–	P: 0.1 MPa, T: 290 K, U_G: 0.1–0.3 m/s	0.19	S	
Behkish et al. [28]	N_2, He	Isopar-M	Alumina	P: 0.7–3.0 MPa, T: 300–453 K, U_G: 0.07–0.39 m/s, C_V: 0–20 vol.%	0.29	S	
Behkish [77]	H_2, N_2, CO, He, CH_4	Isopar-M	Glass beads, Alumina	P: 0.17–3.00 MPa, T: 298–453 K, U_G: 0.06–0.39 m/s, C_V: 0–36 vol.%	0.29, 0.316	S	
Inga [78]	H_2, CO, CH_4, N_2	Hexanes	Iron oxides	P: 0.126–0.767 MPa, T: ambient, U_G: 0.06–0.35 m/s, C_V: 0–21.76 vol.%	0.316	S	
Li et al. [70]	Air	Water	Glass beads	P: atm., T: ambient, U_G: 0.05–0.3 m/s	0.28	S	
Sehabiague et al. [79]	H_2, N_2	Sasol wax, Isopar-M	Alumina, iron oxides	P: 0.17–3.00 MPa, T: 298–453 K, U_G: 0.06–0.39 m/s, C_V: 0–20 vol.%	0.29	S	

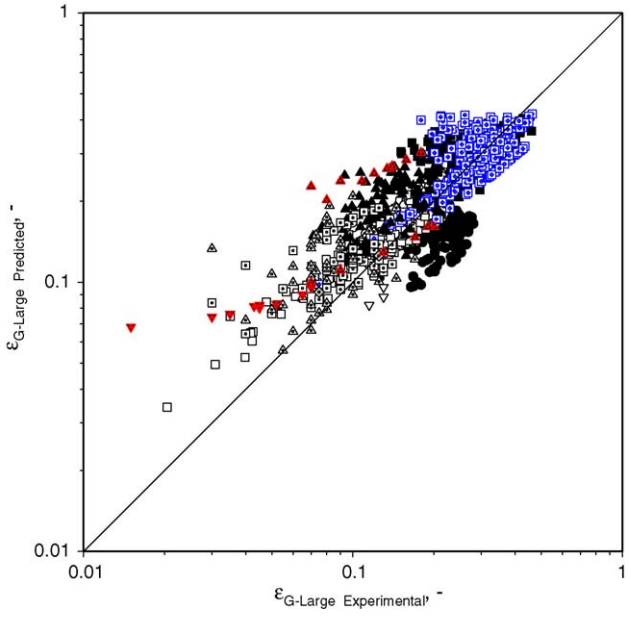

Fig. 2. Comparison between predicted and experimental large gas bubbles holdup data using Eq. (4).

1. If ε_G is $\leq (F)^{25/4}$, small gas bubbles do not exist; Eq. (4) cannot be used to split ε_G into $\varepsilon_{G\text{-Large}}$ and $\varepsilon_{G\text{-Small}}$.
2. If, ε_G is $>(F)^{25/4}$ small and large gas bubbles coexist; Eqs. (1) and (4) can be used.

4. Gas holdup prediction/analysis using the novel correlations

4.1. Prediction of the gas holdup using Eq. (1) and available literature correlations

The literature correlations listed in Table 1 along with Eq. (1) were used to predict the total gas holdup data obtained in BCR and SBCR.

Fig. 3 shows a comparison between the predicted and experimental total gas holdup data obtained by Lemoine et al. [1] for N_2 in a mixture of toluene-benzoic acid-benzaldehyde aimed at simulating the liquid-phase toluene oxidation process in BCRs. As can be clearly seen in this figure most of available literature correlations fail to predict the experimental gas holdup values, whereas the predictions using Eq. (1) are in a very good agreement. This is because only the new correlation takes into account the effect of liquid-phase composition on the total gas

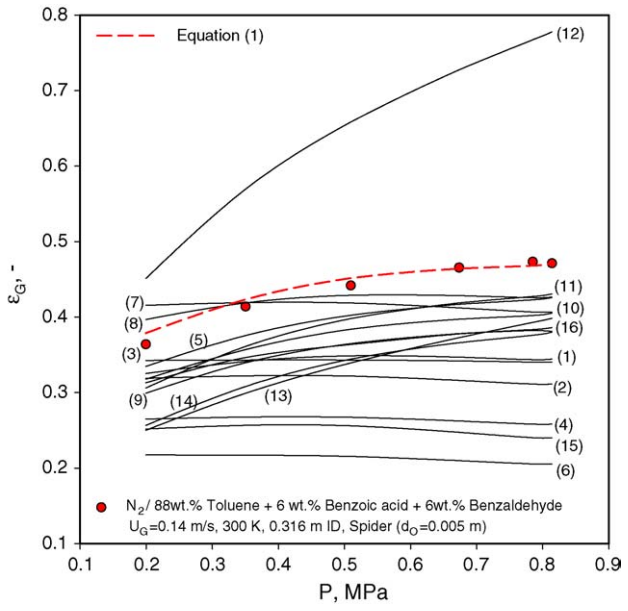

Fig. 3. Prediction of the experimental data by Lemoine et al. [1] obtained in a BCR using Eq. (1) and the available literature correlations in Table 1: (1) Hikita et al. [3], (2) Bach and Pilhofer [2], (3) Kumar et al. [8], (4) Hughmark [4], (5) Reilly et al. [9], (6) Zou et al. [13], (7) Sauer and Hempel [16], (8) Idogawa et al. [5], (9) Fan et al. [14], (10) Jordan and Schumpe [6], (11) Wilkinson et al. [12], (12) Krishna and Sie [15], (13) Krishna and Ellenberger [7], (14) Urseanu et al. [11], (15) Schumpe et al. [17], (16) Reilly et al. [10].

holdup as in the system employed by Lemoine et al. [1]. Fig. 4 shows a comparison between the experimental total gas holdup data obtained by Behkish and Morsi [80] for H_2 in Isopar-M, containing 36 vol.% of glass beads and those predicted using the correlations given in Table 1 proposed for SBCRs. As can be observed in this figure, literature correlations used do not predict the effect of solid concentration on the gas holdup of H_2 in Isopar-M/glass beads slurry. Eq. (1), on the other hand, shows the best fit within AARE and σ of 12 and 10%, respectively.

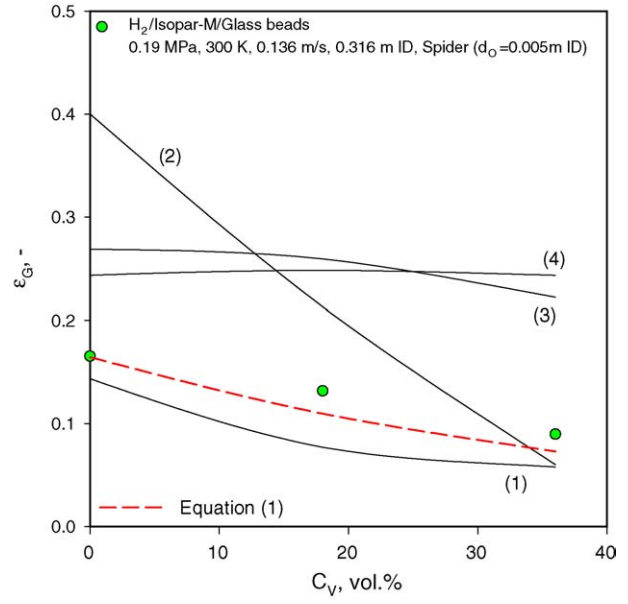

Fig. 4. Prediction of experimental data of Behkish and Morsi [80] using available published correlations developed for SBCR from Table 1 and Eq. (1): (1) Fan et al. [14], (2) Krishna and Sie [15], (3) Sauer and Hempel [16], (4) Schumpe et al. [17].

4.2. Prediction of the effect of operating variables on the total gas holdup in a Fischer–Tropsch slurry reactor using Eq. (1)

The importance of Fischer–Tropsch (F–T) slurry technology stems from the fact that it is a vital venue for producing environmentally acceptable ultra-clean fuels (sulfur-free) which might alleviate the world dependency on oil consumption. This imperative need for the development of F–T slurry technology can be demonstrated by the numerous worldwide activities, such as: (1) Exxon's pilot-scale SBCR (1.2 m diameter, 21 m height) in Baton Rouge, Louisiana [15,81] with 200 bbl/day capacity using Exxon's proprietary cobalt and ruthenium-based catalysts [82]; (2) Rentech Inc. pilot-scale SBCR (1.83 m diameter, 16.7 m height) in Pueblo, Colorado with 500 bbl/day capacity using iron-based catalyst [82]; (3) Sasol's commercial SBCR (5 m diameter, 22 m height) in South Africa with 2500 bbl/day capacity using iron oxides catalyst [83].

Eq. (1) was used to predict the effects of pressure, temperature, gas velocity, rector size, and distributor type on the total gas holdup for syngas (CO and H_2) in Fischer–Tropsch wax using

Table 7
Typical systems and conditions for Fischer–Tropsch synthesis in SBCRs [15,30,66,78,79,83]

Operating conditions	
Pressure (MPa)	2–5
Temperature (K)	473–530
Superficial gas velocity (m/s)	0.05–0.4
Catalyst concentration (vol.%)	5–35
Gas/liquid/solid system	
Gas	
H_2	$M_A = 2.02$ kg/kmol
CO	$M_A = 28.01$ kg/kmol
H_2/CO ratio	2
Liquid	
Wax (n-C_{17}-C_{79})	$M_B = 567.4$ kg/kmol
Density	ρ_L (493 K) = 706 kg/m^3
	ρ_L (513 K) = 696 kg/m^3
Viscosity	μ_L (493 K) = 4.41×10^{-3} Pa s
	μ_L (513 K) = 4.04×10^{-3} Pa s
Surface tension	σ_L (493 K) = 18×10^{-3} N/m
	σ_L (513 K) = 17×10^{-3} N/m
Composition	$X_W = 1.0$
Solid	
Alumina powder	Support for cobalt catalyst
Density	$\rho_P = 3218.3$ kg/m^3
Particle size	$d_P = 42 \times 10^{-6}$ m
Reactor geometry	
Column diameter	0.1–5 m
Height/diameter	4–20
Sparger type	M-ON, S
Orifice diameter	0.01–0.03 m
We_{min}	10

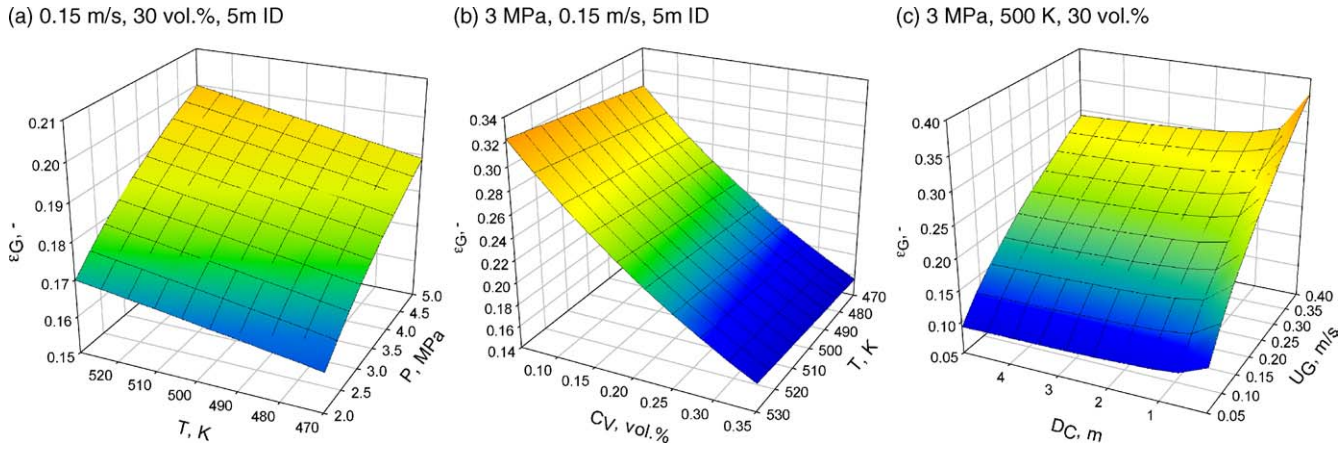

Fig. 5. Effect of the operating variables and reactor size on the total syngas holdup in wax under Fischer–Tropsch conditions (M-ON, d_O = 0.02 m i.d.).

SBCRs of different sizes, operating under typical F–T conditions [15,30,66,78,79,83] as summarized in Table 7. It should be noted that these predictions are solely valid for non-reactive systems since the typical industrial operating conditions of F–T slurry reactors are well within the limits of the variables given in Table 4, which were used to develop Eq. (1).

Fig. 5(a–c) shows the effect of the operating conditions and slurry reactor geometry on the gas holdup of a syngas having a $H_2/CO = 2$ in wax under typical Fischer–Tropsch conditions; and as can be seen ε_G increases with increasing pressure, temperature, superficial gas velocity and decreases with increasing catalyst concentration, which is in agreement with literature findings [1,3,6,7,10,12,14,28,34,55,67,69,78]. This figure shows that under the following conditions: 3 MPa, 493 K, 0.15 m/s, 30 vol.% of alumina-supported cobalt catalyst in a 5 m i.d. column and a multiple orifice nozzle gas distributor with 0.02 m i.d. orifice, the syngas holdup in wax is about 18%. This relatively low gas holdup can be attributed to the small density of the syngas used (7.82 kg/kmol) and the relatively high catalyst loading which led to bubbles coalescence and froth reduction [14,16,28].

Fig. 5(c) shows the effect of the internal diameter of the SBCR on the total gas holdup under the following condition: 3 MPa, 500 K, 30 vol.% of alumina-supported cobalt catalyst and a multiple orifice nozzle gas distributor with 0.02 m i.d. orifice; and as can be observed the total gas holdup decreases by 17% when the reactor diameter increases from 0.1 to 0.8 m and then levels off. Also, the total gas hold up appears to decrease by 22% when the

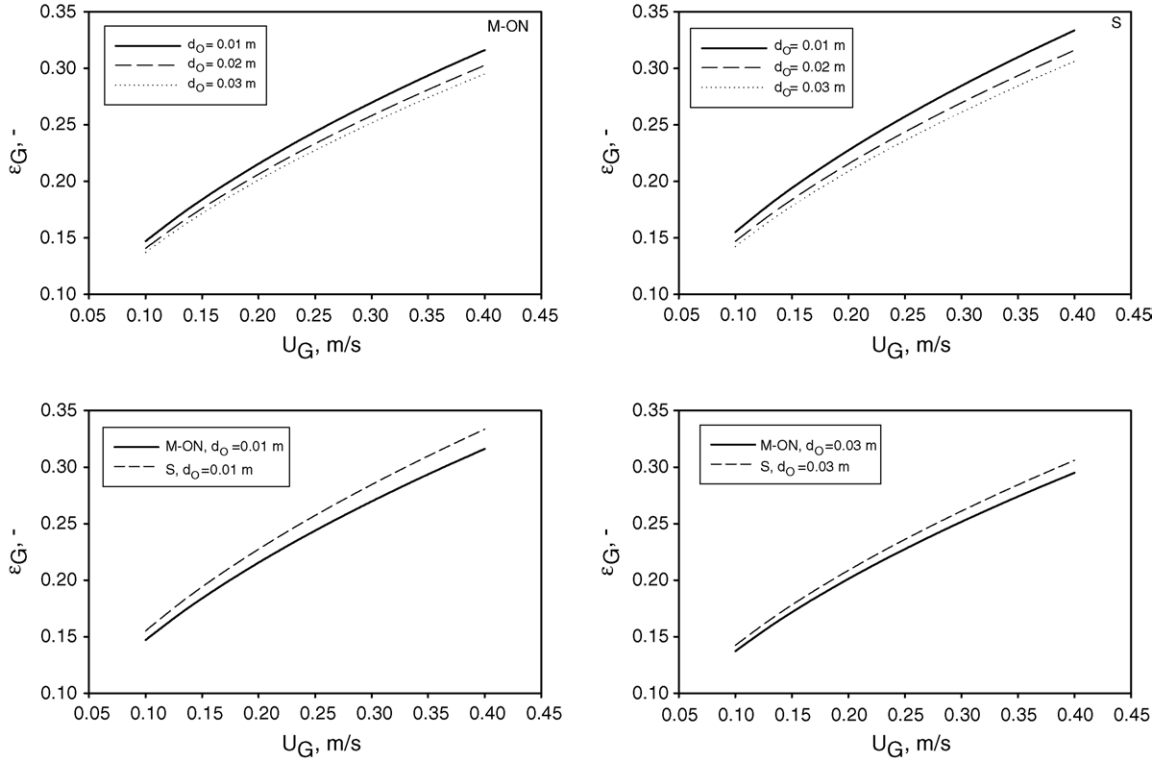

Fig. 6. Effect of gas sparger on the total gas holdup of syngas, (H_2/CO = 2/1) in wax using Eq. (1) (3 MPa, 500 K, 30 vol.%, 5 m i.d., We_{min} = 10).

reactor diameter is increased from 0.1 to 5 m i.d., indicating a non-negligible dependency of the total gas holdup on the inside diameter of SBCRs.

4.3. Prediction of the effect of gas distributor design on the total gas holdup in a Fischer–Tropsch slurry reactor using Eq. (1)

Eq. (1) was also used to predict the effect of gas distributor-type on the total gas holdup in SBCR, operating under typical non-reactive Fisher–Tropsch conditions. Two different gas distributors, a multiple-orifice nozzle and a spider-type gas distributor were used. Since the diameter (d_O) and the number (N_O) of orifices affect the total gas holdup, the diameter of the orifice was fixed at a given value, whereas the number of orifices was calculated based on the orifice Weber number (We_G) defined as

$$We_G = \frac{\rho_G U_{G,O}^2 d_O}{\sigma_L} = \frac{\rho_G U_G^2 D_C^4}{N_O^2 d_O^3 \sigma_L} \quad (6)$$

Under the conditions studied, an arbitrary $We_G = 10$ at the minimum superficial gas velocity used was assumed to calculate the number of orifices (N_O) from Eq. (7), since it has been reported that when We_G is greater than 2, the bubble breakage and axial mixing in the slurry are enhanced [30].

$$N_O = \sqrt{\frac{\rho_G U_{G,min}^2 D_C^4}{10 d_O^3 \sigma_L}} \quad (7)$$

Fig. 6 illustrates that for the multiple-orifice nozzle and the spider-type gas distributor the ε_G decreases with increasing orifice diameter. For instance ε_G appears to decrease by 4.3 and 6.7% and by 5.3 and 8.2% for the multiple-orifice nozzle and spider-type distributor with increasing the orifice diameter from 0.01 to 0.02 and from 0.01 to 0.03 m, respectively. Although these increases seem insignificant, the trend indicates that large gas bubbles are formed with the larger orifice diameter and consequently lower total gas holdup was predicted.

Fig. 6 also shows that the total gas holdup obtained with the spider-type distributor is consistently greater than that with a multiple-orifice nozzle which can be attributed to the more even gas distribution achieved with the spider-type sparger. This difference between the gas holdups by the two distributors, however, is about 5.5 and 3.8% for 0.01 and 0.03 m orifice diameter, respectively which is small.

4.4. Prediction of large and small gas bubbles holdup in a Fischer–Tropsch slurry reactor using Eqs. (4) and (5)

Fig. 7 shows the effect of solid concentration, C_V, and superficial gas velocity, U_G, on the total holdup along with those of large and small bubbles of syngas ($H_2/CO = 2$) in wax under typical Fischer–Tropsch conditions. As can be seen in this figure increasing catalyst concentration from 0 to 14 vol.% decreases the holdup of small gas bubbles whereas that of large gas bubbles remains almost unchanged. At catalyst concentration greater than 14 vol.%, the holdup of small gas bubbles vanishes and

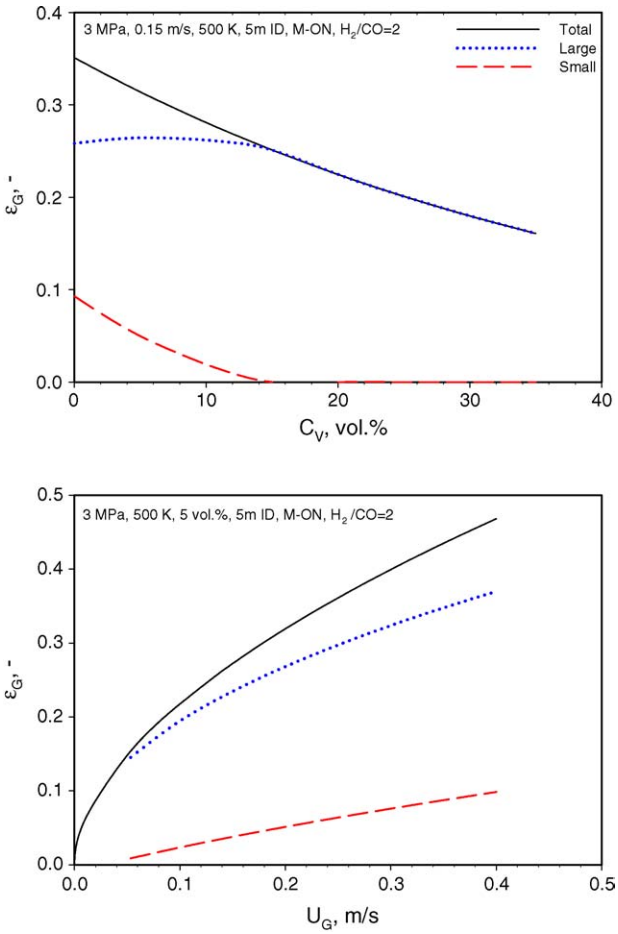

Fig. 7. Effect of C_V and U_G on the holdup of large and small bubbles of syngas in wax under Fischer–Tropsch conditions using Eqs. (1), (4) and (5).

that of large gas bubbles start to decrease due to the enhancement of the coalescence of gas bubbles with increasing the slurry viscosity. Such a behavior is in agreement with the available literature [15,28] and should be considered in modeling of SBCRs for Fischer–Tropsch synthesis.

Fig. 7 also shows that increasing the superficial gas velocity (U_G) increases both the holdup of small and large gas bubbles. At low U_G (<0.04 m/s), however, it seems that the reactor operates in the homogeneous (bubbly) flow regime where only one-class of gas bubbles exists; accordingly the gas bubbles cannot be split into small and large. At $U_G \geq 0.04$ m/s, the gas bubbles interaction increases and the frequency of gas bubble breakup is enhanced [12,19], indicating a heterogeneous (churn-turbulent) flow regime. In fact, when U_G increases from 0.05 to 0.4 m/s, the total gas holdup ε_G is doubled; however, $\varepsilon_{G\text{-Small}}$ is increases 11 times, which underlines the importance of considering both small and large gas bubbles in modeling, design, and scaleup of SBCRs.

5. Conclusions

Two novel correlations were developed using our gas holdup data and those available in the literature obtained for different gases in various liquids and slurries using bubble columns and

slurry bubble column reactors operating under wide ranges of conditions in different size reactors provided with a variety of gas distributors. The correlations were able to predict the experimental data within good absolute average relative error (AARE) and standard deviation (σ). The novel correlations were also used to predict the gas holdup in BCRs and SBCRs, and to study the effects of pressure, temperature, gas velocity, rector size, and distributor type on the gas holdup for syngas ($H_2/CO = 2$) in Fischer–Tropsch wax using SBCRs of different sizes. The gas holdup predictions using the novel correlations led to the following conclusions:

1. In a 5-m i.d. SBCR provided with a multiple orifice nozzle gas distributor (0.02 m i.d. orifice), operating under typical non-reactive Fischer–Tropsch conditions: syngas ($H_2/CO = 2$), wax (n-$C_{17\text{-}79}$), pressure (3 MPa), temperature (493 K), superficial gas velocity (0.15 m/s), alumina-supported cobalt catalyst concentration (30 vol.%) with particle mean diameter ($d_P = 42 \times 10^{-6}$ m) in a 5 m i.d. column, the total syngas holdup was about 18%.
2. The total syngas holdup increased with pressure, superficial gas velocity, temperature and decreased with increasing catalyst concentration. The total gas holdup was also found to slightly decrease with increasing column diameter until about 0.8 m i.d. and then leveled off.
3. The total syngas holdups obtained with the multiple-orifice nozzle and the spider-type gas distributor decreased with increasing orifice diameter. Also, the total gas holdup obtained with the spider-type distributor was systematically greater than that with a multiple-orifice nozzle under similar conditions.
4. The decrease of syngas holdup with increasing catalyst concentration was due to the decrease of holdup of small gas bubbles which disappeared at catalyst concentration of about 14 vol.%. The disappearance of small gas bubbles under such conditions was attributed to the increase of gas bubbles coalescence due to the increase of slurry viscosity.

References

[1] R. Lemoine, A. Behkish, B.I. Morsi, Hydrodynamic and mass transfer characteristics in organic liquid mixture in a large-scale bubble column reactor for toluene oxidation process, Eng. Chem. Res. 43 (2004) 6195–6212.

[2] H.F. Bach, T. Pilhofer, Variations of gas hold-up in bubble columns with physical properties of liquids and operating parameters of column, Ger. Chem. Eng. 1 (1978) 270–275.

[3] H. Hikita, S. Asai, K. Tanigawa, K. Segawa, M. Kitao, Gas hold-up in bubble columns, Chem. Eng. J. 20 (1980) 59–67.

[4] G.A. Hughmark, Holdup and mass transfer in bubble columns, Ind. Eng. Chem. Process Des. Dev. 6 (1967) 218–220.

[5] K. Idogawa, K. Ikeda, T. Fukuda, S. Morooka, Effect of gas and liquid properties on the behavior of bubbles in a column under pressure, Int. Chem. Eng. 27 (1987) 93–99.

[6] U. Jordan, A. Schumpe, The gas density effect on mass transfer in bubble columns with organic liquids, Chem. Eng. Sci. 56 (2001) 6267–6272.

[7] R. Krishna, J. Ellenberger, Gas holdup in bubble column reactors operating in the churn-turbulent flow regime, AIChE J. 42 (1996) 2627–2634.

[8] A. Kumar, T.E. Degaleesan, G.S. Laddha, H.E. Hoelscher, Bubble swarm characteristics in bubble columns, Can. J. Chem. Eng. 54 (1976) 503–508.

[9] I.G. Reilly, D.S. Scott, T.J.W. de Bruijn, A. Jain, J. Piskorz, A correlation for gas holdup in turbulent coalescing bubble columns, Can. J. Chem. Eng. 64 (1986) 705–717.

[10] I.G. Reilly, D.S. Scott, T.J.W. de Bruijn, D. MacIntyre, The role of gas phase momentum in determining gas holdup and hydrodynamic flow regimes in bubble column operations, Can. J. Chem. Eng. 72 (1994) 3–12.

[11] M.I. Urseanu, R.P.M. Guit, A. Stankiewicz, G. van Kranenburg, J.H.G.M. Lommen, Influence of operating pressure on the gas hold-up in bubble columns for high viscous media, Chem. Eng. Sci. 58 (2003) 697–704.

[12] P.M. Wilkinson, A.P. Spek, L.L. van Dierendonck, Design parameters estimation for scale-up of high-pressure bubble columns, AIChE J. 38 (1992) 544–554.

[13] R. Zou, X. Jiang, B. Li, Y. Zu, L. Zhang, Studies on gas holdup in a bubble column operated at elevated temperature, Ind. Eng. Chem. Res. 27 (1988) 1910–1916.

[14] L.S. Fan, G.Q. Yang, D.J. Lee, K. Tsuchiya, X. Luo, Some aspects of high-pressure phenomena of bubbles in liquid and liquid–solid suspensions, Chem. Eng. Sci. 54 (1999) 4681–4709.

[15] R. Krishna, S.T. Sie, Design and scale-up of the Fischer–Tropsch bubble column slurry reactor, Fuel Process. Technol. 64 (2000) 73–105.

[16] T. Sauer, D.C. Hempel, Fluid dynamics and mass transfer in a bubble column with suspended particles, Chem. Eng. Technol. 10 (1987) 180–189.

[17] A. Schumpe, A.K. Saxena, L.K. Fang, Gas/liquid mass transfer in a slurry bubble column, Chem. Eng. Sci. 42 (1987) 1787–1796.

[18] S.S. Ozturk, A. Schumpe, W.-D. Deckwer, Organic liquids in a bubble column: holdups and mass transfer coefficients, AIChE J. 33 (1987) 1473–1480.

[19] J.R. Inga, B.I. Morsi, Effect of operating variables on the gas holdup in a large-scale slurry bubble column reactor operating with organic liquid mixture, Ind. Eng. Chem. Res. 38 (1999) 928–937.

[20] D. Bhaga, B.B. Pruden, M.E. Weber, Gas holdup in bubble column containing organic liquid mixtures, Can. J. Chem. Eng. 49 (1971) 417–420.

[21] E. Sada, H. Kumazawa, C.H. Lee, Chemical absorption in a bubble column loading concentrated slurry, Chem. Eng. Sci. 38 (1983) 2047–2051.

[22] A. Behkish, Z. Men, J.R. Inga, B.I. Morsi, Mass transfer characteristics in a large-scale slurry bubble column reactor with organic liquid mixtures, Chem. Eng. Sci. 57 (2002) 3307–3324.

[23] J.S. Gopal, M.M. Sharma, Mass transfer characteristics of low H/D bubble columns, Can. J. Chem. Eng. 61 (1983) 517–526.

[24] J.H.J. Kluytmans, B.G.M. van Wachem, B.F.M. Kuster, J.C. Schouten, Gas holdup in a slurry bubble column: influence of electrolyte and carbon particles, Ind. Eng. Chem. Res. 40 (2001) 5326–5333.

[25] S.C. Saxena, N.S. Rao, P.R. Thimmapuram, Gas phase holdup in slurry bubble column for two- and three-phase systems, Chem. Eng. J. 49 (1992) 151–159.

[26] A. Colmenares, M. Sevilla, J.J. Goncalves, D. Gonzales-Mendizabel, Fluid-dynamic study in a bubble column with internals, Int. Commun. Heat Mass Transfer 28 (2001) 389–398.

[27] G. Quicker, A. Schumpe, W.-D. Deckwer, Gas–liquid interfacial areas in a bubble column with suspended solids, Chem. Eng. Sci. 39 (1984) 179–183.

[28] A. Behkish, R. Lemoine, L. Sehabiague, R. Oukaci, B.I. Morsi, Gas holdup and bubble size behavior in a large-scale slurry bubble column reactor operating with an organic liquid under elevated pressures and temperatures, Chem. Eng. J., 2005, submitted for publication.

[29] R. Lau, W. Peng, G. Velazquez-Vargas, G.Q. Yang, L.S. Fan, Gas–liquid mass transfer in high-pressure bubble columns, Ind. Eng. Chem. Res. 43 (2004) 1302–1311.

[30] W.-D. Deckwer, Bubble Column Reactors, John Wiley and Sons, Chichester, England, 1992.

[31] B.N. Thorat, K. Kataria, A.V. Kulkarni, J.B. Joshi, Pressure drop studies in bubble columns, Ind. Eng. Chem. Res. 40 (2001) 3675–3688.

[32] F. Kastanek, J. Zahradnik, J. Kratochvil, J. Cermak, Modeling of large-scale bubble column reactors for non-ideal gas–liquid systems, in: L.K. Doraiswamy, R.A. Mashelkar (Eds.), Frontier in Chemical Reaction Engineering, vol. 1, John Wiley and Sons, New Delhi, India, 1984, pp. 330–344.
[33] A. Sarrafi, M. Jamialahmadi, H. Muller-Steinhagen, J.M. Smith, Gas holdup in homogeneous and heterogeneous gas–liquid bubble column reactors, Can. J. Chem. Eng. 77 (1999) 11–21.
[34] R. Krishna, J.W.A. de Swart, J. Ellenberg, G.B. Martina, C. Maretto, Gas holdup in slurry bubble columns: effect of column diameter and slurry concentrations, AIChE J. 43 (1997) 311–316.
[35] L.Z. Pino, R.B. Solari, S. Siquier, L. Antonio Estevez, M.M. Yepez, A.E. Saez, Effect of operating conditions on gas holdup in slurry bubble columns with a foaming liquid, Chem. Eng. Commun. 117 (1992) 367–382.
[36] H. Eickenbusch, P.-O. Brunn, A. Schumpe, Mass transfer into viscous pseudoplastic liquid in large-diameter bubble columns, Chem. Eng. Process. 34 (1995) 479–485.
[37] K. Koide, A. Takazawa, M. Komura, H. Matsunaga, Gas holdup and volumetric liquid-phase mass transfer coefficient in solid-suspended bubble columns, J. Chem. Eng. Jpn. 17 (1984) 459–466.
[38] Y.T. Shah, B.G. Kelkar, S.P. Godbole, W.-D. Deckwer, Design parameters estimations for bubble column reactors, AIChE J. 28 (1982) 353–379.
[39] K. Akita, F. Yoshida, Gas holdup and volumetric mass transfer coefficient in bubble columns, Ind. Eng. Chem. Process Des. Dev. 12 (1973) 76–80.
[40] K. Koide, S. Morooka, K. Ueyama, A. Matsuura, F. Yamashita, S. Iwamoto, Y. Kato, H. Inoue, M. Shigeta, S. Suzuki, T. Akehata, Behavior of bubbles in large scale bubble column, J. Chem. Eng. Jpn. 12 (1979) 98–104.
[41] K. Akita, F. Yoshida, Bubble size, interfacial area, and liquid-phase mass transfer coefficient in bubble columns, Ind. Eng. Chem. Process Des. Dev. 13 (1974) 84–91.
[42] J.J. Heijnen, K. Van't Riet, Mass transfer, mixing and heat transfer phenomena in low viscosity bubble column reactors, Chem. Eng. J. 28 (1984) B21–B42.
[43] E. Camarasa, C. Vial, S. Poncin, G. Wild, N. Midoux, J. Bouillard, Influence of coalescence behaviour of the liquid and of gas sparging on hydrodynamics and bubble characteristics in a bubble column, Chem. Eng. Process. 38 (1999) 329–344.
[44] K. Schügerl, J. Lücke, U. Oels, Bubble column bioreactors, Adv. Biochem. Eng. 7 (1977) 1–84.
[45] D.B. Bukur, J.G. Daly, Gas hold-up in bubble columns for Fischer–Tropsch synthesis, Chem. Eng. Sci. 42 (1987) 2967–2969.
[46] J. Chabot, H.I. Lasa, Gas holdups and bubble characteristics in a bubble column operated at high temperature, Ind. Eng. Chem. Res. 32 (1993) 2595–2601.
[47] J.G. Daly, S.A. Patel, D.B. Bukur, Measurement of gas holdups and Sauter mean bubble diameters in bubble column reactors by dynamic gas disengagement method, Chem. Eng. Sci. 47 (1992) 3647–3654.
[48] I. Dewes, A. Küksal, A. Schumpe, Gas density effect on mass transfer in three-phase sparged reactors, TransIChemE 73 (1995) 697–700.
[49] G.S. Grover, C.V. Rode, R.V. Chaudhari, Effect of temperature on flow regime and gas holdup in a bubble column, Can. J. Chem. Eng. 64 (1986) 501–504.
[50] G. Grund, A. Schumpe, W.-D. Deckwer, Gas–liquid mass transfer in a bubble column with organic liquids, Chem. Eng. Sci. 47 (1992) 3509–3516.
[51] B. Halard, Y. Kawase, M. Moo-Young, Mass transfer in a pilot plant scale airlift column with non-Newtonian fluids, Ind. Eng. Chem. Res. 28 (1989) 243–245.
[52] P. Jiang, T.-J. Lin, X. Luo, L.S. Fan, Flow visulaization of high pressure (21 MPa) bubble column: bubble characteristics, Trans IChemE 73 (1995) 269–274.
[53] H. Kataoka, H. Takeuchi, K. Nakao, H. Yagi, T. Tadaki, T. Otake, T. Miyauchi, K. Washimi, K. Watanabe, F. Yoshida, Mass transfer in a large bubble column, J. Chem. Eng. Jpn. 12 (1979) 105–110.
[54] A. Laari, J. Kallas, S. Palosaari, Gas–liquid mass transfer in bubble columns with a T-junction nozzle for gas dispersion, Chem. Eng. Technol. 20 (1997) 550–556.
[55] H.M. Letzel, J.C. Schouten, C.M. van den Bleek, R. Krishna, Influence of elevated pressure on the stability of bubbly flows, Chem. Eng. Sci. 52 (1997) 3733–3739.
[56] S.F. Moujaes, Internal R&D Task Summary Report: Large-scale Dissolver Cold-Flow Modeling, DOE report # DOE/OR/03054-20, 1984.
[57] L.R.Z. Pino, M.M. Yepez, A.E. Saez, Hydrodynamics of a semibatch slurry bubble column with a foaming liquid, AIChE J. 36 (1990) 1758–1762.
[58] R. Pohorecki, W. Moniuk, A. Zdrojkowski, P. Bielski, Hydrodynamics of a pilot plant bubble column under elevated temperature and pressure, Chem. Eng. Sci. 56 (2001) 1167–1174.
[59] Y.T. Shah, S. Joseph, D.N. Smith, J.A. Ruether, On the behavior of the gas phase in a bubble column with ethanol–water mixtures, Ind. Eng. Chem. Process Des. Dev. 24 (1985) 1140–1148.
[60] S.R. Syeda, A. Afacan, K.T. Chuang, Prediction of gas hold-up in a bubble column filled with pure and binary liquids, Can. J. Chem. Eng. 80 (2002) 44–50.
[61] B. Tarmy, M. Chang, C. Coulaloglou, P. Ponzi, Hydrodynamic characteristics of three phase reactors, Chem. Eng. 407 (1984) 18–23.
[62] G.D. Towell, C.P. Strand, G.H. Ackerman, Mixing and mass transfer in large-diameter bubble columns, Proc. AIChE-Inst. Chem. Eng. 10 (1965) 97–105.
[63] U.P. Veera, K.L. Kataria, J.B. Joshi, Gas hold-up in foaming liquids in bubble columns, Chem. Eng. J. 84 (2001) 247–256.
[64] H. Wezorke, Einflüss von Grössblasen in Blasensäulenreaktoren, PhD Dissertation, University of Dortmund, Germany, 1986.
[65] P.M. Wilkinson, H. Haringa, L.L. Van Dierendonck, Mass transfer and bubble size in a bubble column under pressure, Chem. Eng. Sci. 49 (1994) 1417–1427.
[66] W.-D. Deckwer, Y. Louisi, A. Zaidi, M. Ralek, Hydrodynamic of the Fischer–Tropsch slurry process, Ind. Eng. Chem. Process. Des. Dev. 19 (1980) 699–708.
[67] X. Luo, D.J. Lee, R. Lau, G. Yang, L.S. Fan, Maximum stable bubble size and gas holdup in high-pressure slurry bubble columns, AIChE J. 45 (1999) 665–680.
[68] K.H. Choi, Y. Chisti, M. Moo-Young, Comparative evaluation of hydrodynamic and gas–liquid mass transfer characteristics in bubble column and airlift slurry reactors, Chem. Eng. J. 62 (1996) 223–229.
[69] B. Gandhi, A. Prakash, M.A. Bergougnou, Hydrodynamic behavior of slurry bubble column at high solids concentrations, Powder Technol. 103 (1999) 80–94.
[70] H. Li, A. Prakash, A. Margaritis, M.A. Bergougnou, Effect of micron-sized particles on hydrodynamics and local heat transfer in a slurry bubble column, Powder Technol. 133 (2003) 177–184.
[71] W. O'Dowd, D.N. Smith, J.A. Ruether, S.C. Saxena, Gas and solids behavior in a baffled and unbaffled slurry bubble column, AIChE J. 33 (1987) 1959–1970.
[72] S.P. Godbole, Study of hydrodynamic and mass transfer characteristics of multiphase bubble column reactor, PhD Dissertation, University of Pittsburgh, Pittsburgh, USA, 1983.
[73] J. Ellenberger, R. Krishna, A unified approach to the scale-up of gas–solid fluidized bed and gas–liquid bubble column reactors, Chem. Eng. Sci. 49 (1994) 5391–5411.
[74] C.L. Hyndman, F. Larachi, C. Guy, Understanding gas-phase hydrodynamics in bubble columns: a convective model based on kinetic theory, Chem. Eng. Sci. 52 (1997) 63–77.
[75] U. Jordan, A.K. Saxena, A. Schumpe, Dynamic gas disengagement in a high-pressure bubble column, Can. J. Chem. Eng. 81 (2003) 491–498.
[76] D. Vermeer, R. Krishna, Hydrodynamics and mass transfer in bubble columns in operating in the churn-turbulent regime, Ind. Eng. Chem. Process Des. Dev. 20 (1981) 475–482.
[77] A. Behkish, Hydrodynamic and Mass Transfer Parameters in Large-scale Slurry Bubble Column Reactors, PhD Dissertation, University of Pittsburgh, USA, 2004.

[78] J.R. Inga, Scaleup and Scaledown of Slurry Reactors: A novel methodology, PhD Dissertation, University of Pittsburgh, USA, 1997.
[79] L. Sehabiague, A. Behkish, R. Lemoine, Y. Heintz, B.I. Morsi, Hydrodynamic and mass transfer parameters of slurry bubble column reactors operating under Fischer–Tropsch conditions, in: Presented at the Annual AIChE meeting, Austin, TX, November 7–12, 2004.
[80] A. Behkish, B.I. Morsi, Hydrodynamic and mass transfer characteristics in a large-scale slurry bubble column operating at high pressure and temperature, in: Presented at the Annual AIChE Meeting, Reno, November 4–9, 2001.
[81] A. Jess, R. Popp, K. Hedden, Fischer–Tropsch-synthesis with nitrogen-rich syngas Fundamentals and reactor design aspects, Appl. Catal. A: Gen. 186 (1999) 321–342.
[82] G.P. Van der Laan, Kinetics, Selectivity and Scale Up of the Fischer–Tropsch Synthesis, PhD dissertation, University of Groningen, The Netherlands, 1999.
[83] B. Jager, R. Espinoza, Advances in low temperature Fischer–Tropsch synthesis, Catal. Today 23 (1995) 17–28.